

New Measurements of the Transverse Beam Asymmetry for Elastic Electron Scattering from Selected Nuclei

S. Abrahamyan,⁴⁸ A. Acha,¹¹ A. Afanasev,¹² Z. Ahmed,³⁵ H. Albataineh,⁷ K. Aniol,³ D. S. Armstrong,⁸ W. Armstrong,³⁷ J. Arrington,¹ T. Averett,⁸ B. Babineau,²⁵ S.L.Bailey,⁸ J. Barber,⁴³ A. Barbieri,⁴⁶ A. Beck,²⁷ V. Bellini,¹⁶ R. Beminiwattha,²⁹ H. Benaoum,³⁵ J. Benesch,³⁸ F. Benmokhtar,⁹ P. Bertin,⁷ T. Bielarski,⁴⁴ W. Boeglin,¹¹ P. Bosted,³⁸ F. Butaru,⁵ E. Burtin,⁵ J. Cahoon,⁴³ A. Camsonne,³⁸ M. Canan,³⁰ P. Carter,⁹ C.C. Chang,⁴² G. D. Cates,⁴⁶ Y.-C. Chao,³⁸ C. Chen,¹³ J.-P. Chen,³⁸ Seonho Choi,³³ E. Chudakov,³⁸ E. Cisbani,¹⁸ B. Craver,¹⁸ F. Cusanno,^{18,*} M. M. Dalton,⁴⁶ R. De Leo,¹⁵ K. de Jager,^{38,46} W. Deconinck,^{27,8} P. Decowski,³⁴ D. Deepa,³⁰ X. Deng,⁴⁶ A. Deur,³⁸ D. Dutta,²⁸ A. Etile,⁷ C. Ferdi,⁷ R. J. Feuerbach,³⁸ J.M. Finn,^{8,†} D. Flay,³⁷ G. B. Franklin,⁴ M. Friend,⁴ S. Frullani,¹⁸ E. Fuchey,^{7,37} S.A. Fuchs,⁸ K. Fuoti,⁴³ F. Garibaldi,¹⁸ E. Gasser,⁷ R. Gilman,^{32,38} A. Giusa,¹⁶ A. Glamazdin,²² L.E. Glesener,⁸ J. Gomez,³⁸ M. Gorchtein,^{19,49} J. Grames,³⁸ K. Grimm,⁸ C. Gu,⁴⁶ O. Hansen,³⁸ J. Hansknecht,³⁸ O. Hen,³⁶ D. W. Higinbotham,³⁸ R. S. Holmes,³⁵ T. Holmstrom,²⁵ C. J. Horowitz,¹⁹ J. Hoskins,⁸ J. Huang,^{27,26} T.B. Humensky,³⁹ C. E. Hyde,^{30,7} H. Ibrahim,^{30,2} F. Itard,⁷ C.-M. Jen,³⁵ E. Jensen,⁸ X. Jiang,^{32,26} G. Jin,⁴⁶ S. Johnston,⁴³ J. Katich,⁸ L.J. Kaufman,^{43,‡} A. Kelleher,²⁷ K. Kliakhandler,³⁶ P.M. King,²⁹ A. Kolarkar,⁴¹ S. Kowalski,²⁷ E. Kuchina,³² K. S. Kumar,⁴³ L. Lagamba,¹⁵ D. Lambert,³⁴ P. LaViolette,⁴³ J. Leacock,⁴⁷ J. Leckey IV,⁸ J. H. Lee,^{8,29,§} J. J. LeRose,³⁸ D. Lhuillier,⁵ R. Lindgren,⁴⁶ N. Liyanage,⁴⁶ N. Lubinsky,³¹ J. Mammei,⁴³ F. Mammoliti,¹⁶ D.J. Margaziotis,³ P. Markowitz,¹¹ M. Mazouz,²³ K. McCormick,³² A. McCreary,³⁸ D. McNulty,⁴³ D.G. Meekins,³⁸ L. Mercado,⁴³ Z.-E. Meziani,³⁷ R. W. Michaels,³⁸ M. Mihovilovic,²⁰ B. Moffit,⁸ P. Monaghan,¹³ N. Muangma,²⁷ C. Muñoz-Camacho,⁷ S. Nanda,³⁸ V. Nelyubin,⁴⁶ D. Neyret,⁵ Nuruzzaman,²⁸ Y. Oh,³³ K. Otis,⁴³ A. Palmer,²⁵ D. Parno,⁴ K. D. Paschke,⁴⁶ S. K. Phillips,^{44,¶} M. Poelker,³⁸ R. Pomatsalyuk,²² M. Posik,³⁷ M. Potokar,²⁰ K. Prok,⁵ A.J.R. Puckett,^{27,26} X. Qian,¹⁰ Y. Qiang,^{27,**} B. Quinn,⁴ A. Rakhman,³⁵ P. E. Reimer,¹ B. Reitz,³⁸ S. Riordan,^{43,46} J. Roche,^{29,38} P. Rogan,⁴³ G. Ron,²⁴ G. Russo,¹⁶ K. Saenboonruang,⁴⁶ A. Saha,^{38,†} B. Sawatzky,³⁸ A. Shahinyan,^{48,38} R. Silwal,⁴⁶ J. Singh,⁴⁶ S. Sirca,²⁰ K. Slifer,⁴⁴ R. Snyder,⁴⁶ P. Solvignon,³⁸ P. A. Souder,^{35,††} M. L. Sperduto,¹⁶ R. Subedi,⁴⁶ M.L. Stutzman,³⁸ R. Suleiman,³⁸ V. Sulkosky,^{27,8} C. M. Sutera,¹⁶ W. A. Tobias,⁴⁶ W. Troth,²⁵ G. M. Urciuoli,¹⁷ P. Ulmer,³⁰ A. Vacheret,⁵ E. Voutier,²³ B. Waidyawansa,²⁹ D. Wang,⁴⁶ K. Wang,⁴⁶ J. Wexler,⁴³ A. Whitbeck,⁴¹ R. Wilson,¹⁴ B. Wojtsekhowski,³⁸ X. Yan,⁴⁵ H. Yao,³⁷ Y. Ye,⁴⁵ Z. Ye,^{13,46} V. Yim,⁴³ L. Zana,³⁵ X. Zhan,¹ J. Zhang,³⁸ Y. Zhang,³² X. Zheng,⁴⁶ V. Ziskin,²⁷ and P. Zhu⁴⁵

(HAPPEX and PREX Collaborations)

¹Argonne National Laboratory, Argonne, Illinois 60439, USA

²Cairo University, Giza 12613, Egypt

³California State University, Los Angeles, Los Angeles, California 90032, USA

⁴Carnegie Mellon University, Pittsburgh, Pennsylvania 15213, USA

⁵CEA Saclay, DAPNIA/SPhN, F-91191 Gif-sur-Yvette, France

⁶China Institute of Atomic Energy, Beijing 102413, China

⁷Clermont Université, Université Blaise Pascal, CNRS/IN2P3,

Laboratoire de Physique Corpusculaire, FR-63000 Clermont-Ferrand, France

⁸College of William and Mary, Williamsburg, Virginia 23187, USA

⁹Christopher Newport University, Newport News, Virginia 23606, USA

¹⁰Duke University, TUNL, Durham, North Carolina, 27706, USA

¹¹Florida International University, Miami, Florida 33199, USA

¹²The George Washington University, Washington DC 20052, USA

¹³Hampton University, Hampton, Virginia 23668, USA

¹⁴Harvard University, Cambridge, Massachusetts 02138, USA

¹⁵INFN, Sezione di Bari and University of Bari, I-70126 Bari, Italy

¹⁶INFN, Sezione di Catania and University of Catania, I-95123 Catania, Italy

¹⁷INFN, Sezione di Roma, I-00161 Rome, Italy

¹⁸INFN, Sezione di Roma, gruppo Sanità, I-00161 Rome, Italy

¹⁹Indiana University, Bloomington, Indiana 47405, USA

²⁰Institut Jožef Stefan, 3000 SI-1001 Ljubljana, Slovenia

²¹Kent State University, Kent, Ohio 44242, USA

²²Kharkov Institute of Physics and Technology, Kharkov 61108, Ukraine

²³LPSC, Université Joseph Fourier, CNRS/IN2P3, INPG, Grenoble, France

²⁴Lawrence Berkeley National Laboratory, Berkeley, California 94720, USA

²⁵Longwood University, Farmville, Virginia 23909, USA

²⁶Los Alamos National Laboratory, Los Alamos, New Mexico 87545, USA

²⁷Massachusetts Institute of Technology, Cambridge, Massachusetts 02139, USA

²⁸Mississippi State University, Mississippi State, Mississippi 39762, USA

²⁹Ohio University, Athens, Ohio 45701, USA

³⁰Old Dominion University, Norfolk, Virginia 23529, USA

³¹Rensselaer Polytechnic Institute, Troy, New York 12180, USA

³²Rutgers University, The State University of New Jersey, New Brunswick, New Jersey 08901, USA

³³Seoul National University, Seoul 151-742, South Korea

³⁴Smith College, Northampton, Massachusetts 01063, USA

³⁵Syracuse University, Syracuse, New York 13244, USA

³⁶Tel Aviv University, P.O. Box 39040, Tel-Aviv 69978, Israel

³⁷Temple University, Philadelphia, Pennsylvania 19122, USA

³⁸Thomas Jefferson National Accelerator Facility, Newport News, Virginia 23606, USA

³⁹University of Chicago, Chicago, Illinois, 60637, USA

⁴⁰University of Illinois, Urbana, Illinois, 61801, USA

⁴¹University of Kentucky, Lexington, Kentucky 40506, USA

⁴²University of Maryland, College Park, Maryland, 20742, USA

⁴³University of Massachusetts Amherst, Amherst, Massachusetts 01003, USA

⁴⁴University of New Hampshire, Durham, New Hampshire 03824, USA

⁴⁵University of Science and Technology of China, Hefei, Anhui 230026, P.R. China

⁴⁶University of Virginia, Charlottesville, Virginia 22903, USA

⁴⁷Virginia Polytechnic Institute and State University, Blacksburg, Virginia 24061, USA

⁴⁸Yerevan Physics Institute, Yerevan, Armenia

⁴⁹Institute für Kernphysik, Universität Mainz, 55128 Mainz, Germany

(Dated: April 11, 2018)

We have measured the beam-normal single-spin asymmetry A_n in the elastic scattering of 1-3 GeV transversely polarized electrons from ^1H and for the first time from ^4He , ^{12}C , and ^{208}Pb . For ^1H , ^4He and ^{12}C , the measurements are in agreement with calculations that relate A_n to the imaginary part of the two-photon exchange amplitude including inelastic intermediate states. Surprisingly, the ^{208}Pb result is significantly smaller than the corresponding prediction using the same formalism. These results suggest that a systematic set of new A_n measurements might emerge as a new and sensitive probe of the structure of heavy nuclei.

PACS numbers: 25.30.Bf, 27.10.+h $A \leq 5$, 27.20.+n $6 \leq A \leq 19$, 27.80.+w $190 \leq A \leq 219$

Traditionally, fixed-target electron scattering has been analyzed in terms of the one-boson (photon or Z) exchange approximation. For scattering off heavy nuclei, distorted waves, based on solutions to the Dirac equation in the strong electric field of the nucleus, are also required to describe the data. Recently, the inclusion of the exchange of one or more additional photons has been necessary for the interpretation of precision data. The electric form factor G_E^p extracted in elastic electron-proton scattering using two different techniques, Rosenbluth separation and polarization observables, were inconsistent [1–3]. The latter should be less sensitive to higher order electromagnetic effects and calculations including two-photon exchange provide a plausible explanation for the difference [4–8]. Another example is corrections to the parity-violating asymmetry A_{PV} in the same process, which provides a measurement of the weak charge of the proton and serves as a sensitive test of the electroweak theory. For interpreting A_{PV} , γ - Z box diagrams are important [9], as well as two-photon exchange [10]. Theoretical calculations of two photon exchange processes are difficult because an integral over all off-shell proton intermediate state contributions must be made.

The effect of the extra boson is relatively small on the

measured cross section or asymmetry for the above examples. On the other hand, the beam-normal spin asymmetry A_n for elastic electron scattering at GeV energies is dominated by two (or more) γ exchange. Several measurements of A_n at GeV energies for the proton have been reported [11–14]. Several theoretical papers report computed values of A_n that are in qualitative agreement with the data when they include the effects of inelastic intermediate hadronic states [15–18].

The beam-normal, or transverse asymmetry, A_n is a direct probe of higher-order photon exchange as time-reversal symmetry dictates that A_n is zero at first Born approximation. Afanasev *et al.* [4] and Gorchtein and Horowitz [19] have calculated A_n , in a two-photon exchange approximation, but including a full range of intermediate excited states. Gorchtein and Horowitz predict that A_n scales roughly as the ratio of mass number A to Z , and is not strongly Z -dependent. In contrast Cooper *et al.* [20] calculate Coulomb distortion effects and work to all orders in photon exchanges by numerically solving the Dirac equation. However, they only consider the elastic intermediate state. They find that elastic intermediate state contributions, while in general small, increase strongly with Z .

Target	H	^4He	^{12}C	^{208}Pb
θ	6°	6°	5°	5°
Q^2 (GeV 2)	0.0989	0.0773	0.00984	0.00881
E_b (GeV)	3.026	2.750	1.063	1.063
$\langle \cos \phi \rangle$	0.968	0.967	0.963	0.967

TABLE I: Kinematic values for the various targets.

To predict A_n for nuclear targets, Afanasev used a unitarity-based model [18] with the total photoproduction cross section and the Compton slope as input; his prediction for ^4He is consistent with the value of A_n reported in this paper. However, there is not yet a calculation of A_n that includes both Coulomb distortion effects and a full range of excited intermediate states. Measuring A_n as a function of Z might reveal the role of dispersion effects relative to Coulomb distortions and motivate more detailed calculations. To this end, in this Letter, we report data on the beam-normal spin-asymmetry A_n on the targets ^1H , ^4He , ^{12}C , and ^{208}Pb .

To observe the beam-normal single-spin asymmetry, the electron beam spin vector \vec{P}_e must have a component normal to the scattering plane defined by the unit vector \hat{k} perpendicular to the plane, where $\hat{k} = \vec{k}/|k|$; $\vec{k} = \vec{k}_e \times \vec{k}_{\text{out}}$, with \vec{k}_e and \vec{k}_{out} are respectively the incident and scattered electron momenta. The measured beam-normal single-spin asymmetry is then defined as $A_n^m = (\sigma_{\uparrow} - \sigma_{\downarrow})/(\sigma_{\uparrow} + \sigma_{\downarrow})$ where $\sigma_{\uparrow(\downarrow)}$ is the cross section for beam electron spin parallel(anti-parallel) to \hat{k} . The measured asymmetry A_n^m is related to A_n by

$$A_n^m = A_n \vec{P}_e \cdot \hat{k}, \quad (1)$$

where ϕ is the angle between \hat{k} and \vec{P}_e : $\cos \phi = \vec{P}_e \cdot \hat{k}/|P_e|$.

The measurements were carried out in Hall A at the Thomas Jefferson National Accelerator Facility. The data were obtained as a part of a study of systematic uncertainties for three experiments designed to measure A_{PV} in elastic electron scattering, since A_n can contribute to the extracted A_{PV} if the beam polarization has a transverse component and the apparatus lacks perfect symmetry.

The data were obtained in 2004 for the ^1H and ^4He targets where the primary goal was to measure A_{PV} in order to determine the strange form factors in the nucleon [21, 22]. The ^{12}C and ^{208}Pb data were obtained in 2010 where the goal was to determine the radius of the distribution of neutrons [23, 24]. The kinematics for each target is given in Table I: the central acceptance angle of the spectrometers θ , the beam energy E_b , the acceptance-averaged 4-momentum transfer Q^2 , and the average accepted $\cos \phi$ (Eqn. 1). The uncertainties in Q^2 were 1% for the ^1H and ^4He data and 1.3% for the ^{12}C and ^{208}Pb data [21–23].

All of the targets except ^{12}C were cooled with helium gas at about 20K. The LH_2 and high pressure He targets

featured rapid vertical flow of the fluid. In addition, the beam was rastered over a $4 \text{ mm} \times 4 \text{ mm}$ square for all targets. The 0.55 mm thick isotopically pure ^{208}Pb target was sandwiched between two $150 \mu\text{m}$ diamond foils, and the edges were cooled with the cold helium. Electrons elastically scattered from the targets were focused onto detectors in the focal plane of the Hall A High Resolution Spectrometers [25]. The transverse asymmetry is modulated by the sine of the azimuthal electron scattering angle and so the electron polarization was set vertical. This ensured that the acceptance of the two spectrometers, which are symmetrically placed to accept horizontally scattered events, contained the maximum and minimum of the asymmetry. The momentum resolution of the spectrometers ensured that essentially only elastic events were accepted.

To measure the asymmetry, Cherenkov light was produced in a radiator and collected by a PMT, whose output sent to an analog-to-digital converter (ADC) and integrated over a fixed time period of constant helicity. These detectors had to withstand the radiation damage caused by the high signal flux and also provide a uniform response to the electrons so that integrating the signals did not increase fluctuations. For the ^{208}Pb and ^{12}C data, each spectrometer had two 3.5 cm by 14 cm quartz detectors oriented at 45° to the direction of the electrons in the spectrometer, one in front that was 5 mm thick and one behind that was 1 cm thick. For the ^1H and ^4He data, a five-layer sandwich of quartz and brass provided sufficient energy resolution.

The electron beam originated from a GaAs photocathode illuminated by circularly polarized light [26]. By reversing the sign of the laser circular polarization, the direction of the spin at the target could be reversed rapidly [27]. A half-wave ($\lambda/2$) plate was periodically inserted into the laser optical path which passively reversed the sign of the electron beam polarization. Roughly equal statistics were thus accumulated with opposite signs for the measured asymmetry, which suppressed many systematic effects. The direction of the polarization could be controlled by a Wien filter and solenoidal lenses near the injector [28]. The accelerated beam was directed into Hall A, where its intensity, energy and trajectory on target were inferred from the response of several monitoring devices.

Each period of constant spin direction is referred to as a “window”. The beam monitors, target, detector components and electronics were designed so that the fluctuations in the fractional difference in the PMT response between a pair of successive windows were dominated by scattered electron counting statistics. To keep spurious beam-induced asymmetries under control at well below the ppm level, careful attention was given to the design and configuration of the laser optics leading to the photocathode [27].

The spin-reversal rate was 30 Hz for the ^1H and ^4He

data and 240 Hz for the ^{12}C and ^{208}Pb data. The integrated response of each detector PMT and beam monitor was digitized and recorded for each window. In the 30 Hz case, the raw spin-direction asymmetry A_{raw} in each spectrometer arm was computed from the the detector response normalized to the beam intensity for each window pair. At the faster reversal, quadruplets of windows with either of the patterns $+-+-$ or $-+ +-$ were used to suppress the significant 60 Hz line noise. In either case, the sequence of these patterns was chosen with a pseudorandom number generator.

Loose requirements were imposed on beam quality, removing periods of beam intensity, position, or energy instability, removing about 25% of the total data sample. No spin-direction-dependent cuts were applied. Since we measure the difference between two horizontal detectors, the dominant source of noise due to the beam arose from position fluctuations in the horizontal direction, which change the acceptance of the spectrometers in opposite directions. Noise in the beam energy or current largely cancels. In contrast, a measurement of the sum of the detectors in the A_{PV} case is relatively more sensitive to beam energy or current fluctuations and less to the beam position.

As explained in detail in [21–23], the window-to-window differences in the asymmetry from beam jitter were reduced by using the correlations to beam position differences from precision beam position monitors, Δx_i by defining a correction $A_{\text{beam}} = \sum c_i \Delta x_i$. The c_i were measured several times each hour from calibration data where the beam was modulated using steering coils and an accelerating cavity. The largest c_i was for ^{208}Pb and was on the order of 50 ppb/nm. The spread in the resulting $A_n^{\text{m}} = A_{\text{raw}} - A_{\text{beam}}$ was observed to be dominated by counting statistics. For example, for ^{208}Pb , which had the highest rate and hence the smallest statistical uncertainty for a window, this spread corresponded to a rate of about 1 GHz at beam current of 70 μA . About one day was spent at each $\lambda/2$ setting on each target.

The values of A_n^{m} were consistent from run-to-run as shown in Fig. 1. The asymmetries in each spectrometer arm were of opposite sign as expected (\hat{k} in Eq. 1 reverses sign). After correcting for the the $\lambda/2$ reversals, the magnitudes of A_n^{m} are consistent within statistical uncertainties. The reduced χ^2 for a constant fit to the A_n^{m} runs is close to one for each target type. The average A_{beam} corrections were negligible. The physics asymmetry A_n is calculated from A_n^{m} by correcting for the beam polarization P_e , the average value of $\cos\phi$ as given in Table I, and the background subtractions from the Al windows in the LH_2 and ^4He targets, and the diamond surrounding the lead foil.

Nonlinearity in the PMT response was limited to 1% in bench tests that mimicked running conditions. The total relative nonlinearity between the PMT response and those of the beam intensity monitors was limited to 1.5%

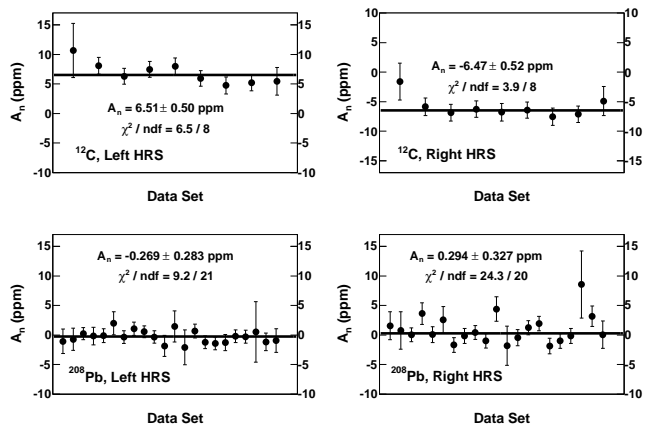


FIG. 1: Plots of the asymmetries for carbon and lead. Top row shows for the ^{12}C target the left-HRS and right-HRS asymmetries in the left and right panels, respectively. Bottom row shows the same sequence for the ^{208}Pb target. The data have been sign-corrected for the $\lambda/2$ plate insertions.

by studies. An acceptance correction accounted for the non-linear dependence of the asymmetry with Q^2 . A significant systematic uncertainty in $\langle Q^2 \rangle$ is in the determination of the absolute scale of θ_{lab} . A nuclear recoil technique with a dedicated calibration run using a water cell target [22] was used to set a scale uncertainty on $\langle Q^2 \rangle$ of $< 0.2\%$.

Beam polarization measurements (P_e in Eq. 1) were made during the runs for the four nuclei. The beam polarization was inferred from longitudinal polarization measurements taken before and after the transverse polarization data taking. A solenoid was used to control the orientation of the polarization between the longitudinal and transverse (vertical) direction. The polarization was verified to be purely vertical to within $\pm 2^\circ$ with a Mott polarimeter located in an injector 5 MeV extraction line. The vertical component of the polarization set at the injector is conserved after passing through the CEBAF accelerator, a result of accelerating and transporting the polarized beam in planes flat with respect to one another. The extent to which the beam-spin tune degrades the vertical polarization orientation in CEBAF has been studied and determined to be $\pm 1^\circ$ [29]. A small longitudinal component of the electron spin introduces a negligible parity-violating contribution to the measured asymmetry.

For ^{12}C and ^{208}Pb , the longitudinal polarization measurements included data taken with a Compton polarimeter, yielding $P_e = 0.8820 \pm 0.012 \pm 0.012$. An independent Møller polarimeter gave $P_e = 0.9049 \pm 0.001 \pm 0.011$ for ^{12}C and ^{208}Pb . We used the average of these two measurements. For the ^1H and ^4He data only the Møller polarimeter was used. For ^1H data, $P_e = 75.1 \pm 1.7\%$ and for the ^4He data, $P_e = 84.2 \pm 1.7\%$.

A summary of the systematic and statistical uncer-

Target	^1H	^4He	^{12}C	^{208}Pb
False asymmetry	0.14	0.11	0.02	0.12
Beam polarization	0.21	0.33	0.08	0.003
Linearity	0.07	0.15	0.06	0.004
Target Windows	0.06	0.12	0.00	0.062
Total Systematic	0.27	0.41	0.10	0.14
Statistical	1.52	1.39	0.36	0.21

TABLE II: A_{PV} uncertainty contributions in units of 10^{-6} or ppm

Target	H	^4He	^{12}C	^{208}Pb
A_n (ppm)	-6.80	-13.97	-6.49	0.28
$\sigma(A_n)$ (ppm)	± 1.54	± 1.45	± 0.38	± 0.25
$\sqrt{Q^2}$ (GeV)	0.31	0.28	0.099	0.094
A/Z	1.0	2.0	2.0	2.53
\hat{A}_n (ppm/GeV)	-21.9	-24.9	-32.8	+1.2
$\sigma(\hat{A}_n)$ (ppm/GeV)	± 5.0	± 2.6	± 1.9	± 1.1

TABLE III: The measured A_n and derived \hat{A}_n values (Eq. 2) for the four nuclei along with the corresponding total uncertainties, A/Z and Q .

ainties is shown in Table II. The central values of A_n for each nucleus and the total combined statistical and systematic uncertainties added in quadrature are displayed in the first two rows of Table III. For ^1H , our result is consistent with a previously reported measurement [12] for the same Q^2 but at a lower beam energy (0.85 GeV).

We now discuss the observed trends of the first ever measurements of A_n for target nuclei with $A > 2$. In our kinematic range, the calculations in ref. [19] scale

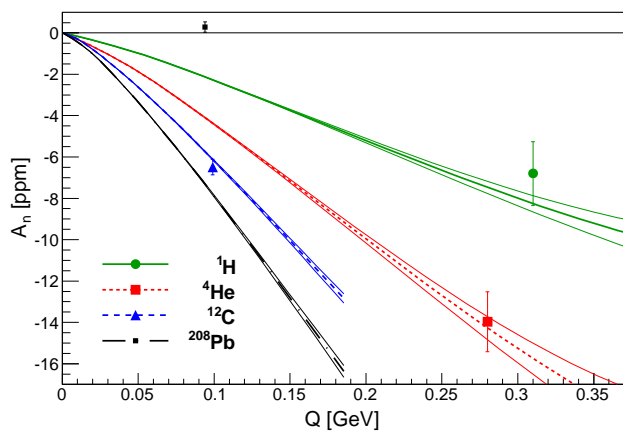


FIG. 2: Extracted physics asymmetries A_n vs. Q . Each curve, specific to a particular nucleus as indicated, is a theoretical calculation from Ref. [19].

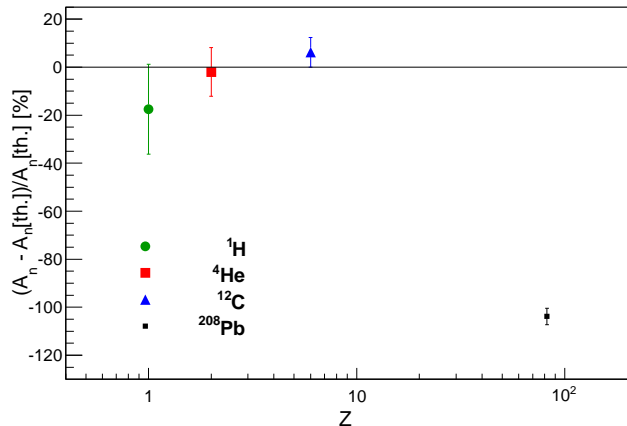


FIG. 3: % fractional deviation of A_n measurements normalized to respective theory prediction vs. target nucleus Z .

approximately with Z , A , and $\sqrt{Q^2}$ as

$$A_n = \hat{A}_n \frac{QA}{Z}, \quad (2)$$

where \hat{A}_n is approximately constant, with a small additional dependence on the incident beam energy E_{beam} : ~ -25 ppm/GeV for $E_{\text{beam}} \sim 3$ GeV (for ^1H and ^4He), and ~ -30 ppm/GeV for $E_{\text{beam}} \sim 1$ GeV (for ^{12}C and ^{208}Pb). In the last two rows of Table III, we see that the extracted \hat{A}_n from the three lower Z nuclei are consistent with this empirical trend, while the ^{208}Pb result is consistent with zero. The ^{208}Pb result is in strong disagreement with the theoretical prediction as shown in Fig. 2, which plots the measurement results and their predictions [19].

Motivated by this large observed disagreement, we initiate a discussion of the potential dynamics by first noting that the scattering angle for all four measurements was roughly the same (Table I). If dispersion corrections play a bigger role than predicted, one might expect larger disagreements for A_n measurements taken at lower beam energy, as is the case for ^{12}C and ^{208}Pb . However, the measured A_n for ^{12}C is quite consistent with theoretical expectations. In Fig. 3, we plot the fractional difference between the measured values and the predictions of Ref. [19] as a function of Z . The trend suggests that Coulomb distortions are playing a very significant role at large Z , underscoring the potential interest in additional A_n measurements with intermediate Z nuclei.

In conclusion, we have measured the beam-normal single-spin asymmetry A_n for ^1H , ^4He , ^{12}C , and ^{208}Pb and find good agreement for ^1H , ^4He and ^{12}C with the calculations in ref. [19], which include a dispersion integral over intermediate excited states. However, they are only to order α^2 (two-photon exchange) and neglect Coulomb distortions. On the other hand, A_n for ^{208}Pb is measured to be very small and disagrees completely

with theoretical calculations. Coulomb distortions were shown in ref. [20] to grow rapidly with Z . On the other hand, the weight of dispersion corrections varies with the incident beam energy. Thus, new theoretical calculations that treat dispersion corrections and Coulomb distortions simultaneously as well as a systematic set of A_n measurements for a range of Z at various beam energies might lead to new insights into the structure of heavy nuclei.

We wish to thank the entire staff of JLab for their efforts to develop and maintain the polarized beam and the experimental apparatus. This work was supported by DOE contract DE-AC05-84ER40150 Modification No. M175, under which the Southeastern Universities Research Association (SURA) operates JLab, contract DE-AC02-06CH11357 for Argonne National Lab, and by the Department of Energy, the National Science Foundation, the INFN (Italy), and the Commissariat à l'Énergie Atomique (France).

* now at Technische Universitaet Muenchen, Excellence Cluster Universe, Garching b. Muenchen, Germany

† Deceased

‡ now at Indiana University, Bloomington, Indiana 47405, USA

§ now at Institute for Basic Science, Daejeon, South Korea

¶ now at University of New Hampshire, Durham, New Hampshire 03824, USA

** now at Thomas Jefferson National Accelerator Facility, Newport News, Virginia 23606, USA

†† Electronic address: souder@physics.syr.edu

- [1] C. F. Perdrisat, V. Punjabi, M. Vanderhaeghen, Prog. Part. Nucl. Phys. **59**, 694 (2007).
- [2] J. Arrington, *et al.* 2007 J. Phys. G: Nucl. Part. Phys. **34**, 23 (2007).
- [3] J. Arrington, Phys.Rev. **C68**, 034325 (2003).
- [4] A. V. Afanasev, S. J. Brodsky, C. E. Carlson, Y. - C. Chen, M. Vanderhaeghen, Phys. Rev. **D72**, 013008 (2005).
- [5] C.E. Carlson, M. Vanderhaeghen, Ann. Rev. Nucl. Part. Sci. **57**, 171 (2007).
- [6] J. Arrington, W. Melnitchouk, J.A. Tjon, Phys. Rev. C **76**, 035205 (2007).
- [7] P.G Blunden, W. Melnitchouk, J.A. Tjon, Phys.Rev. **C72**, 034612 (2005).
- [8] J. Arrington, P.G. Blunden, W. Melnitchouk, Prog.Part.Nucl.Phys. **66**, 782 (2011).
- [9] M. Gorchtein, C. J. Horowitz, M. J. Ramsey-Musolf, Phys. Rev. Lett **C84**, 015502 (2011).
- [10] A.V.Afanasev, C.E. Carlson, Phys. Rev. Lett **94**, 212301 (2005).
- [11] S. P. Wells *et al.* Phys. Rev. **C63**, 064001 (2001).
- [12] F. E. Maas *et al.*, Phys. Rev. Lett. **94**, 082001 (2005).
- [13] D. S. Armstrong *et al.*, Phys. Rev. Lett. **99**, 092301 (2007).
- [14] D. Androic *et al.*, Phys. Rev. Lett. **107**, 022501 (2011).
- [15] A. V. Afanasev, N. P. Merenkov, Phys. Lett. **B599**, 48 (2004).
- [16] B. Pasquini, M. Vanderhaeghen, Eur. Phys. J. **A24S2**, 29-32 (2005).
- [17] B. Pasquini, M. Vanderhaeghen, Phys. Rev. **C70**, 045206 (2004).
- [18] A. V. Afanasev, arXiv 0711.3065 [hep-ph].
- [19] M. Gorchtein, C. J. Horowitz, Phys. Rev. **C77**, 044606 (2008).
- [20] E. D. Cooper, C. J. Horowitz, Phys. Rev. **C72**, 034602 (2005).
- [21] A. Acha *et al.*, Phys. Rev. Lett. **98**, 032301 (2007).
- [22] K. A. Aniol *et al.*, Phys. Rev. Lett. **96**, 022003 (2006).
- [23] S. Abrahamyan *et al.* (PREX Collaboration), Phys. Rev. Lett. **108**, 112502 (2012).
- [24] C.J. Horowitz, S.J. Pollock, P.A. Souder, R. Michaels, Phys. Rev. C **63**, 025501 (2001).
- [25] J. Alcorn *et al.* NIM A **522**, 294 (2004).
- [26] C. K. Sinclair *et al.* Phys. Rev. ST Accel. Beams **10**, 023501 (2007); J. Hansknecht *et al.* Phys. Rev. ST Accel. Beams **13**, 010101 (2010).
- [27] K. D. Paschke, Eur. Phys. J. A **32**, 549 (2007).
- [28] J. Grames, *et al.*, "Two Wien Filter Spin Flipper" in Proceedings of the 2011 Particle Accelerator Conference, New York, New York (2011).
- [29] J.M. Grames, PhD Thesis, "Measurement of a Weak Polarization Sensitivity to the Beam Orbit of the CE-BAF Accelerator", Jefferson Laboratory, JLAB-R-00-001 (January, 2000).